DEVELOPMENT OF A CAMERA-BASED SÖDERBERG ELECTRODE SLIP MEASUREMENT DEVICE

[1]D. T. Jordan, [2]C. J. Hockaday

Mintek, 200 Malibongwe Drive, Randburg, South Africa;
e-mails:[1] dominicj@mintek.co.za, [2] chrish@mintek.co.za

ABSTRACT

One of the most critical parameters to electrode management of submerged-arc furnaces is balancing the electrode slipping rates against consumption. Reliable electrode slip measurement is important in maintaining this balance and is also necessary to ensure that correct electrode baking schedules are adhered to in order to avoid unnecessary electrode breaks. In practice, the harsh conditions in the electrode environment often results in the failure of traditional electromechanical instruments, and thus most plants often default to subjective manual slip measurement techniques.

Mintek has recently developed a patented device, SlipCam, that uses a camera as the primary sensor that continuously monitors the movement of the electrode and slip ring. Computer vision and image processing techniques are then used to process the images to determine electrode slip. This is done by first correcting for the image distortion caused by the camera lens. Strong "features" are then extracted and tracked on both the electrode and slip ring and subsequently processed and filtered to yield a metric slip measurement. Electrode features are attributed to existing points on the steel casing, while slip ring features are extracted from a unique marker applied during installation. Dust and vibration are also accounted for in the algorithm, for improved robustness. Cameras have the distinct advantage in that they are non-contact and non-intrusive to the process. They are also not as susceptible to the dusty environments as alternative measurement devices, such as lasers and ultrasonic sensors.

Industrial testing of the SlipCam shows that the camera performs well in the environment, only requiring minimal attention during scheduled maintenance shutdowns. Tests indicate that the SlipCam is able to account for slips that took place, with an accuracy of greater than 94% over extended periods.

KEYWORDS: *Submerged-Arc Furnace; Slip Measurement; Söderberg Electrode; Camera; Computer Vision.*

1. INTRODUCTION

One of the most critical parameters in the management of Söderberg electrodes in the ferroalloy industry is balancing the electrode slipping rate against consumption. Access to a reliable electrode slip measurement is vital in maintaining this balance and is also necessary to ensure that correct electrode baking schedules are adhered to in order to avoid unnecessary electrode breaks and ultimately furnace downtime. In practice, the harsh conditions in the electrode environment often result in the failure of traditional wheel-based encoders, and thus most plants default to subjective manual slip measurement techniques.

Industrial computer vision based systems have become increasingly popular in recent years [1-3], and have been successfully deployed in numerous ore sorting applications within the mining industry [4]. The use of cameras as sensors is advantageous since they are non-intrusive to the process of interest. In many mining applications, computer vision systems are chosen over the

alternatives due to reliability concerns associated with the harsh environmental conditions. Laser-based sensors often fail in dusty environments and high electromagnetic interference levels might influence the robustness of other non-contact sensors. Ever-increasing computing power, coupled with recent developments in ruggedized high definition cameras, makes computer vision systems increasingly attractive for application to the mining industry.

Mintek has recently developed a patented device, SlipCam, that uses a remotely mounted camera as the primary sensor to continuously monitor the movement of the furnace electrode and slip rings. Computer vision and image processing techniques are used to process the images, yielding a metric slip measurement. This paper discusses the design and development of the SlipCam prototype device and the results achieved during industrial testing.

2. PLANT INFRASTRUCTURE

SLIP SEQUENCE

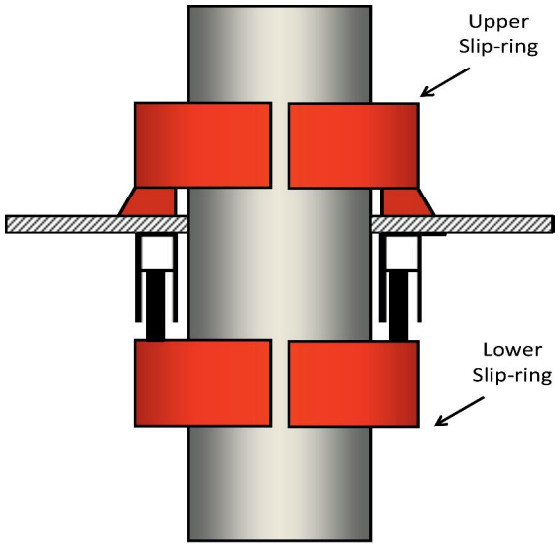

Figure 1: Test site slip ring configuration

Electrode slipping methods vary from furnace to furnace, but tend to follow the same basic sequence. The electrode column at the test site shown in

Figure 1 above consists of an upper and lower slip ring located on different floors in the furnace superstructure. The upper slip ring is fixed relative to the ground. The lower slip ring is mounted on a pair of hydraulic hoists inversely mounted to the floor above. During normal electrode regulation, the upper clamp remains open. During electrode slip, the sequence is as follows:

1. The upper slip ring engages the electrode.
2. The lower slip ring releases its grip on the electrode.
3. The hoists suspending the lower slip ring move upwards, effectively moving the electrode downward through the slip ring.
4. The lower slip ring re-engages the electrode.
5. The upper slip ring releases the electrode.

3. SLIPCAM DESIGN AND IMPLEMENTATION

3.1. SLIP MEASUREMENT TECHNIQUE

In order to continuously monitor the electrode and slip ring within the camera's field of view (FOV), it is necessary to mount the camera in such a way that the slip ring is always visible throughout the vertical travel range of the hoist. Slip can then be calculated by monitoring and measuring relative longitudinal movement between the electrode and slip ring. In order to achieve the desired camera FOV shown in figure 2 below, the camera needs to be mounted to a fixed structure near the electrode and lower slip ring. Once the device has been calibrated, depth perception is not a concern since the perpendicular distance between the camera sensor and the electrode scene remain static. As a result, only a single camera is required.

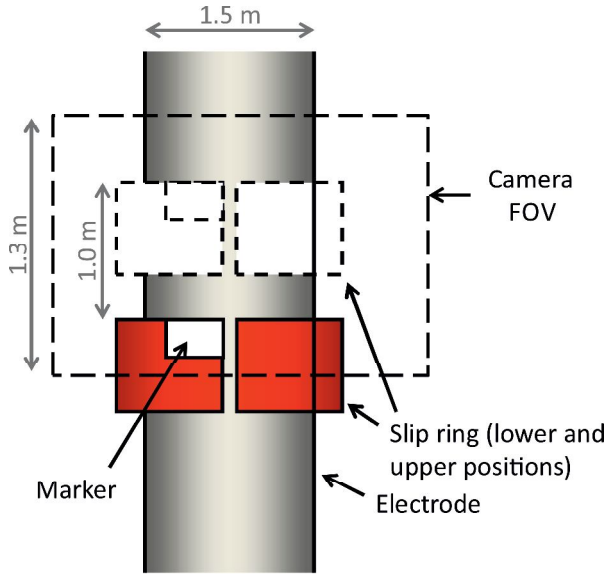

Figure 2: SlipCam camera FOV

3.2. CALIBRATION

A unique marker is placed on the slip ring during device installation for more robust identification of the slip ring against the electrode casing, as shown in figure 2 above. The Speeded-Up-Robust-Features (SURF) [6] corresponding to this reference marker are extracted and stored in memory for future reference.

Lens distortion is present to some extent in all cameras, mainly attributed to manufacturing imperfections, and needs to be removed prior to calculating slip. This is achieved by taking various images of a planar calibration chequer-grid with known geometric dimensions once the camera focus and zoom settings have been configured and locked. Images containing this calibration grid with different orientations are processed to calculate the camera distortion coefficients, which are then used to remove lens distortion in subsequently captured images using the well-established Zhang calibration method [4].

The relationship between the pixels in the image and the corresponding millimetres on the electrode casing are naturally dependent on the distance between the camera and the electrode. It is therefore necessary to calibrate the camera in order to determine a mapping between the pixel and

metric displacement for both the electrode and the slip ring. This is achieved by applying a temporary magnetic calibration chequer strip with known grid dimensions on the electrode during installation, as shown in

Figure 3 below. The location of the corners of the squares and the geometric size of the grids can then be used to produce a pixel to metric map.

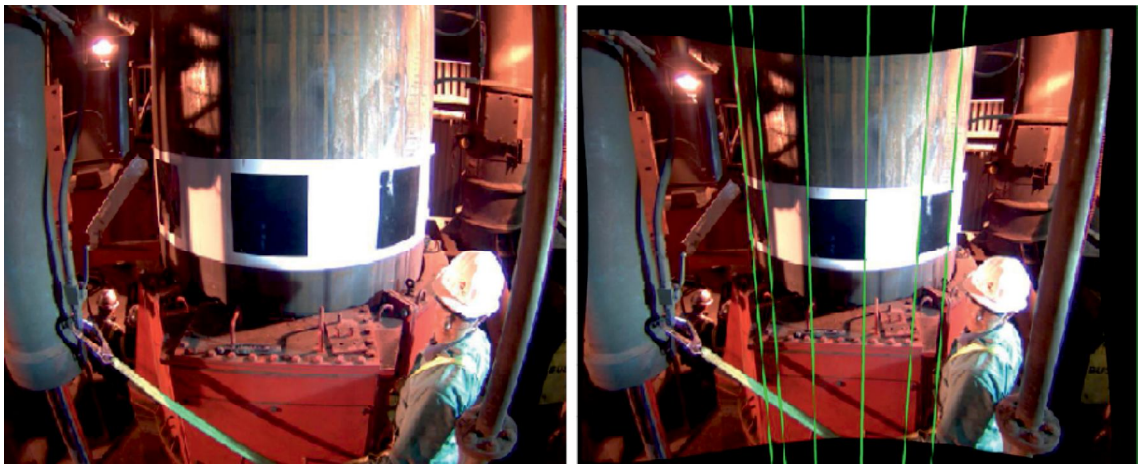

Figure 3: Electrode and slip ring calibration

3.3. SLIP DETERMINATION

The basic slip measurement algorithm used to calculate slip between frames is achievable through the steps shown in figure 4 below.

The steps below are followed in order to calculate metric slip between two images:

Step 1: Removing lens distortion: Lens distortion is removed using the coefficients determined during calibration.

Step 2: Assess image quality: In the harsh furnace environment, furnace over pressures might lead to intermittent increases in dust levels surrounding the electrode. Furthermore, small vibrations of the camera can cause blurring of captured images. For this reason, image quality is analysed before any further analysis is done. Part of this is determining the image blur metric [10] to detect for motion blur. Image histogram analysis is also performed to determine if image dust levels are too high to reliably calculate slip.

Step 3: Segmenting the electrode and slip ring regions of interest: This step involves identifying the regions of interest (ROI) in the image, namely the electrode and the slip ring marker. Since the electrode is periodically slipped, electrode features present in the frame will dynamically change as the electrode passes through the scene. The first task is to extract all SURF features in the image. The SURF matching strategy described in Bay et al [6] is used to match the features found on the reference slip ring marker with features determined during device installation. Further details of this matching strategy will be described in *Step 5*. Using the location of the detected slip ring, the next task is to segment the electrode to account for varying depth from the camera. This is done by using a combination of the Canny edge detection algorithm [7], the probabilistic Hough line transform, and least square linear fitting.

Step 4: Extracting Frame Features: Once the slip ring and the electrode ROI are located, distinct image features corresponding to the two regions are then extracted.

Step 5: Perform feature matching: Once the relative features are found, feature matching of both the electrode and slip ring marker can be performed between the present image and the previous one, using the feature matching strategy given by Bay et al [6].

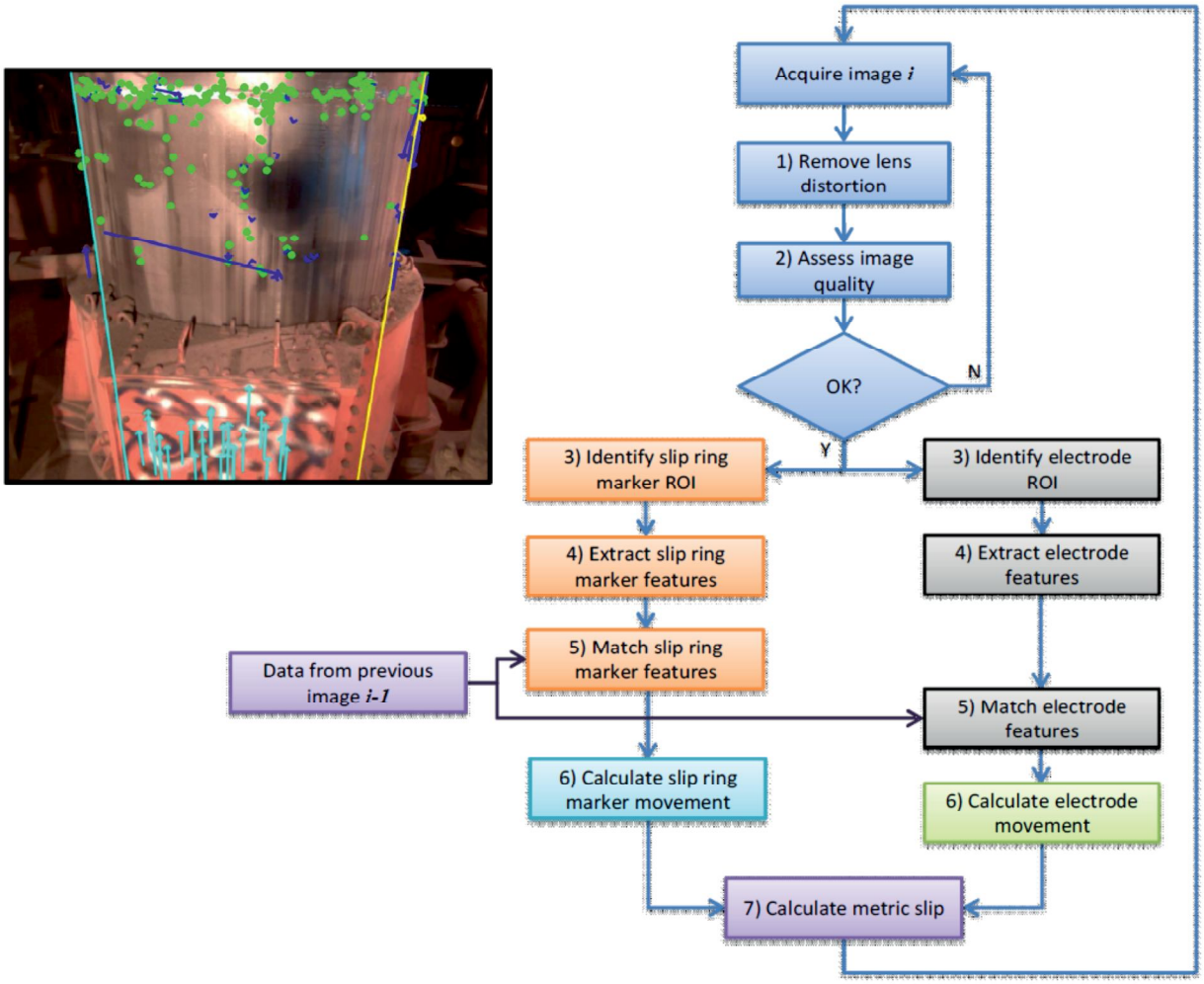

Figure 4: Simplified slip measurement algorithm and typical feature matching result

This effectively tracks electrode and slip ring movement between the two frames. The nature of the extraction and matching strategy used by the device is such that it is relatively robust to reasonable dust and illumination level changes – conditions that can be expected in the furnace environment. This matching step produces sets of feature displacement vectors for the electrode and slip ring respectively. A typical example can be seen in figure 4 above.

Step 6: Calculate average metric slip ring and marker movement: Using the pixel mapping determined during calibration, each feature displacement vector on both the electrode and slip ring is converted to a metric measurement, which is then subsequently filtered and averaged to yield the electrode and slip ring metric displacement between the two frames.

Step 7: Calculate metric slip: Slip is calculated by subtracting the electrode movement from the slip ring movement determined in the previous step. This approach calculates only slip measurement, as normal vertical electrode movement will cause no relative movement between the electrode and the slip ring.

3.4. HARDWARE

Image processing is generally computationally intensive, and a dedicated PC is required to process the images. Furthermore, a ruggedized camera is required in order to withstand the harsh furnace conditions around the electrodes. Power and camera communication should ideally take place over the same channel to simplify the installation process. Ruggedized high definition CCTV

cameras have become increasingly popular in recent years and often use power over Ethernet (POE) technology where camera power and communication both utilise a single conventional category 5 Ethernet cable.

In this application a dome camera is preferable to conventional box-shaped cameras, since the inverted dome minimises dust build-up. The dome camera shown in Figure below was mounted on one of the feed chutes adjacent the electrode at the test site.

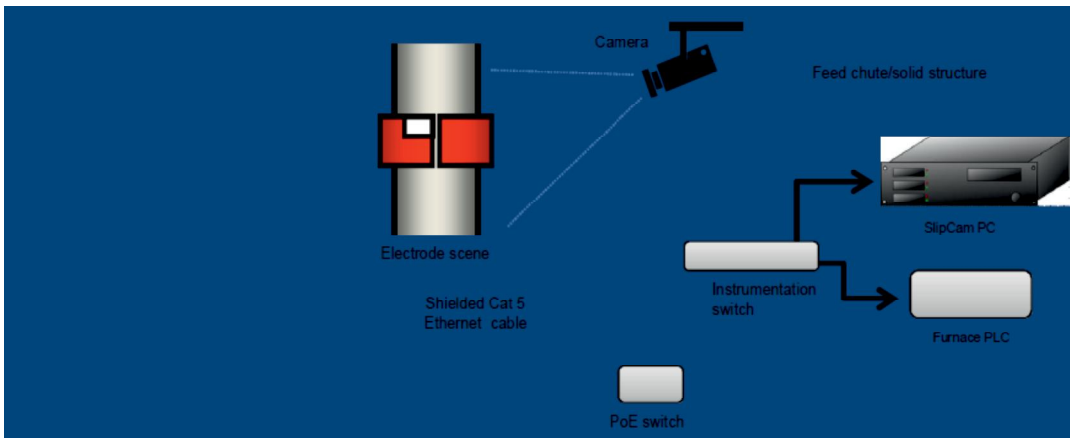

Figure 5: Camera installation relative to the electrode and feed chute (left) and connection to plant infrastructure (right)

The camera is connected to a POE switch located in a PLC marshalling cabinet near the slip rings. The plant network infrastructure was used to connect the camera to the SlipCam PC located in the control room. The SlipCam PC periodically captures the images, processes them, and sends the resultant slip measurement to the furnace control PC for logging purposes and/or writing to the plant PLC.

4. RESULTS

4.1. HARDWARE PERFORMANCE

The SlipCam camera has been installed on site for a period exceeding a year without any hardware performance or reliability issues. Although the dome camera minimises dust settlement, it is recommended that the camera dome housing should be wiped clear at least bi-annually during routine maintenance to remove minor dust build up.

4.2. SLIP MEASUREMENT RESULTS

The challenge in evaluating any new slip measurement device is the poor availability of a reliable reference which can be used as a baseline reference. Ultimately, the most reliable reference is accurate manual electrode marking and measuring. However, cumulative error issues may arise if the overall long term slip measurement is based on accumulating the manually measured individual slips, since millimetre precision is difficult to achieve using chalk markings. For this reason, the following method was used to achieve a reasonably accurate baseline measurement to monitor slip over extended periods:

1) Using the slip/holder position reference pointer on the casing floor, make a distinct horizontal mark on the electrode with permanent marker, ensuring that a rigid object is used to extrapolate the reference to the electrode casing.

2) Make another clear horizontal mark on the electrode as high on the casing as possible.

3) Accurately measure the vertical distance between the markings made in steps 1 and 2 above.

4) Note the distance in step 3, and the measurement time.

5) Depending on the vertical distance measured in step 3, and the average slipping rate, repeat steps 1-4 above every few days, ensuring that the vertical distance between the reference marker and the mark made in previous iterations is also noted. Use these distances to calculate the total slip over the test period.

Using the method mentioned above, a reference slip measurement of 2 070 mm was physically measured on the electrode over a period of 6 consecutive days. During this period, approximately 70 controlled slips were executed by the operator, with no noticeable uncontrolled slips. The SlipCam measurements over the same period produced an accumulated slip of 1 957 mm, which equates to an overall error of less than 5.6%.

During this period, SlipCam also successfully filtered out 6 poor images attributed to motion blur, and one poor image containing too much dust. All hoist movements (normal electrode regulation, not related to slip) were also successfully rejected by the SlipCam algorithm.

Figure 6 below shows SlipCam tracking the recorded operator slip over the period in question. These results fall comfortably within the initial maximum 10% error requirement set by Mintek during the initial feasibility analysis.

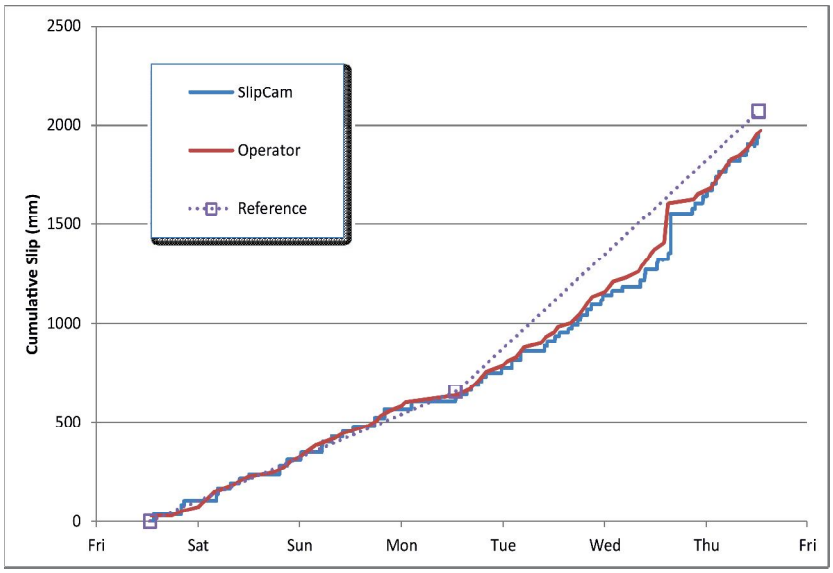

Figure 6: Cumulative Slip

During earlier prototype testing, the overall SlipCam accuracy was monitored over numerous 8 hour periods, since ferroalloy producers are usually interested in total slip from shift to shift. The reference slip measurement was obtained using a similar process to the one mentioned above, where slip was measured on the electrode casing using electrode marks before and after each eight hour shift period.

The results shown in table 1 below indicate that the SlipCam performs with an average error of approximately 4.8%, again well within target accuracy. Electrode hoist positions at the test site are measured using rope encoders, an instrument commonly used at most ferroalloy plants for this purpose. The slip distance is determined by noting the difference in hoist measurement before and after a slip takes place.

The results obtained over both short and medium term show that the SlipCam is capable of identifying and resolving electrode slip into a measurable metric, with accuracy suitable to industrial application. This accuracy is set to increase further with the on-going improvements to the filtering and processing algorithms.

Table 1: Comparison of accuracies of the various slip measurement techniques over full shifts

Slip measurement type	Average absolute error, mm	Standard Deviation, mm	Percentage average, %
Operator slip measurement	1.75	5.32	4.69
Difference in hoist position	11.00	6.22	12.26
SlipCam	3.29	8.95	4.83

5. CONCLUSION

Increasing computing power of desktop computers coupled with the evolution of complex image processing algorithms has facilitated the development of a long sought-after alternative to traditional electrode slip measurement techniques and instruments.

By using optical technology the effects of the unforgiving conditions encountered by conventional slip measurement encoders are mitigated. Long term site testing shows that the only necessary maintenance requirement is bi-annual cleaning of the camera dome housing to minimise dust settlement, which can readily be incorporated into scheduled furnace downtime.

During initial feasibility analysis, Mintek set the overall accuracy requirement at 10% as a baseline for determining whether the SlipCam had the potential to be a feasible measurement alternative. Numerous tests in varying conditions yield show SlipCam to perform comfortably with an error of less than 6%.

With the flexibility afforded by a computer-based measurement solution, this accuracy will only improve in time as filtering and processing algorithms are refined further. The result is a smart instrument capable of measuring electrode slip to a high degree of accuracy, which does not require direct contact with the electrodes.

6. ACKNOWLEDGEMENTS

This paper is published by permission of Mintek. Gratitude is also expressed to Xstrata Boshoek for allowing the use of their furnace, and for their invaluable assistance during installation and testing.

7. REFERENCES

[1] E. Malamas, E. Petrakis, M. Zervakis, L. Petit, and J. Legat, “A survey on industrial vision systems, applications and tools,” Image and Vision Computing, vol. 21, no. 2, pp. 171–188, 2003.

[2] M. L. Smith and L. N. Smith, “Special issue on machine vision”, Computers in Industry, vol. 56, no. 8-9, pp. 773 – 776, 2005.

[3] H. Golnabi and A. Asadpour, “Design and application of industrial machine vision systems,” Robotics and Computer-Integrated Manufacturing, vol. 23, no. 6, pp. 630–637, 2007.

[4] TOMRA Sorting Solutions, available from http://www.tomrasorting.com/mining/, accessed 23 January 2013.

[5] Z. Zhang, "A flexible new technique for camera calibration," IEEE Trans. Pattern Anal. Mach. Intell., vol. 22, no. 11, pp. 1330–1334, 2000.
[6] H. Bay, A. Ess, T. Tuytelaars, and L. Van Gool, "Speeded-up robust features (SURF)," Computer Vision and Image Understanding, vol. 110, no. 3, pp. 346–359, 2008.
[7] J. Canny, "A computational approach to edge detection," IEEE Trans. Pattern Anal. Mach. Intell., vol. 8, no. 6, pp. 679–698, 1986.
[8] J. Matas, C. Galambos, and J. Kittler, "Robust detection of lines using the progressive probabilistic Hough transform," Computer Vision and Image Understanding, vol. 78, no. 1, pp. 119–137, 2000.
[9] Lowe, D. "Object recognition from local scale-invariant features", International Journal of Computer Vision, 60(2), pp 91-110., 1999.
[10] Marziliano, P.; Dufaux, F.; Winkler, S.; Ebrahimi, T.; , "A no-reference perceptual blur metric," Image Processing. 2002. Proceedings. 2002 International Conference on , vol.3, no., pp. III-57- III-60 vol.3, 2002.